Am J Transl Res 2016;8(11):4869-4880
www.ajtr.org /ISSN:1943-8141/AJTR0036873

Original Article

High fructose causes cardiac hypertrophy via mitochondrial signaling pathway

Yan-Bo Zhang, Yan-Hai Meng, Shuo Chang, Rong-Yuan Zhang, Chen Shi

Research Center of Cardiovascular Diseases, State Key Laboratory of Cardiovascular Disease, Fuwai Hospital, National Center for Cardiovascular Diseases, Chinese Academy of Medical Sciences and Peking Union Medical College, Beijing 100037, People's Republic of China

Received July 29, 2016; Accepted October 3, 2016; Epub November 15, 2016; Published November 30, 2016

Abstract: High fructose diet can cause cardiac hypertrophy and oxidative stress is a key mediator for myocardial hypertrophy. Disruption of cystic fibrosis transmembrane conductance regulator (CFTR) leads to oxidative stress. This study aims to reveal mitochondrial oxidative stress-related signaling pathway in high fructose-induced cardiac hypertrophy. Mice were fed high fructose to develop cardiac hypertrophy. Fructose and H_2O_2 were used to induce cardiomyocyte hypertrophy in vitro. Mitochondria-targeted antioxidant SkQ1 was applied to investigate the possible role of mitochondrial reactive oxygen species (ROS). CFTR silence was performed to detect the role of CFTR in high fructose-induced myocardial hypertrophy. ROS, glutathione (GSH), mitochondrial function and hypertrophic markers were measured. We confirmed that long-term high fructose diet caused cardiac hypertrophy and diastolic dysfunction and elevated mitochondrial ROS. However, SkQ1 administration prevented heart hypertrophy and mitochondrial oxidative stress. Cadiomyocytes incubated with fructose or H_2O_2 exhibited significantly increased cell areas but SkQ1 treatment ameliorated cardiomyocyte hypertrophy induced by high fructose or H_2O_2 in vitro. Those results revealed that the underlying mechanism for high fructose-induced heart hypertrophy was attributed to mitochondrial oxidative stress. Moreover, CFTR expression was decreased by high fructose intervention and CFTR silence resulted in an increase in mitochondrial ROS, which suggested high fructose diet affected mitochondrial oxidative stress by regulating CFTR expression. Electron transport chain impairment might be related to mitochondrial oxidative damage. In conclusion, our findings indicated that mitochondrial oxidative stress plays a central role in pathogenesis of high fructose-induced cardiac hypertrophy. High fructose decreases CFTR expression to regulate mitochondrial oxidative stress.

Keywords: Fructose, cardiac hypertrophy, mitochondria, oxidative stress, cystic fibrosis transmembrane conductance regulator

Introduction

Dietary fructose intake has increased sharply in recent decades and this has been paralleled by an increase in the incidence of cardiovascular diseases such as cardiac hypertrophy, hypertension and insulin resistance. A high-fat and high-sucrose diet leads to metabolic heart disease with left ventricular hypertrophy (LVH) and diastolic dysfunction [1, 2]. Long-term dietary fructose intervention induces systemic glucose dysregulation and cardiac hypertrophic response including markedly enlarged heart, increased heart coefficient and abundantly swelled cardiomyocyte area [3]. It has been reported that the development of LVH can be affected by diet manipulation and LVH resulting from pressure overload becomes worse by high fructose feeding [4, 5].

Oxidative stress is a potential link between high carbohydrate intake and heart disease progression. Mitochondria have been considered as one most important source of reactive oxygen species (ROS) such as O_2^- and H_2O_2 which could result in damage to the organelle in cells [6, 7]. Emerging evidence suggest that mitochondrial ROS play a very important role in the development of cardiac hypertrophy [1, 6, 8, 9]. Antioxidant treatment such as tempol, resveratrol, and polyphenolic families could prevent biochemical cardiovascular changes and cardiac hypertrophy in high-fructose-fed animal models [5, 10, 11]. Recently, the development

of mitochondria-targeted antioxidant strongly facilitates the studies on the role of mitochondrial ROS in pathophysiological processes [12-14]. Mitochondria-targeted plastoquinone SkQ1 prevents nephropathy and brain damage induced by ischemia injury and it also improves impaired dermal wound healing in old mice by scavenging mitochondrial ROS [15-17]. Some studies report elevated mitochondrial ROS level is closely associated with dysfunctional cystic fibrosis transmembrane conductance regulator (CFTR) which is a low-conductance, cAMP-regulated and ATP-gated chloride channel and has been observed in a variety of cell types including heart cells and vascular smooth muscle cells [18, 19].

In this study, we hypothesized that mitochondrial oxidative stress mediated high fructose-induced cardiac hypertrophy and CFTR loss induced by high fructose diet contributed to mitochondrial oxidative stress. We firstly assessed the impact of a long-term high fructose diet on LVH and then explored the potential mechanism for high fructose-induced cardiac hypertrophy.

Materials and methods

Animals

Male C57BL/6 mice with 8-10 weeks of age were randomly divided into four groups: 1) control group (Con); 2) SkQ1 group; 3) high fructose group (FS); 4) FS+SkQ1 group. Control mice were given standard chow diet and normal drinking water for 20 weeks while mice in FS group received standard chow diet and 10% fructose water by adding 10 g fructose into 100 ml drinking water for 20 weeks [20]. Mitochondria-targeted antioxidant SkQ1 (100 nmol/kg/d) was administered in drinking water for SkQ1 and FS+SkQ1 groups [15]. SkQ1 reagent used in this study was purchased from Sigma. Mice were weighed and killed at the end of the study. The protocol was approved by the Animal Care and Use Committee of Chinese Academy of Medical Sciences and Peking Union Medical College.

Echocardiography and doppler

Echocardiography was performed using a Vevo 2100 Imaging System (VisualSonics, Canada) with 12.5-45 MHz linear transducer as previously described [21]. Mice were continuously anesthetized by isoflurane inhalant (1.0-1.5% in oxygen). The heart was first imaged in B-mode in the parasternal long axis view and then M-mode image was obtained by placing the M-mode sample gate perpendicularly to the interventricular septum (IVS) and left ventricular wall at the level of papillary muscle. Parasternal short axis image in B-mode and M-mode were obtained at the level of papillary muscle. M-mode from long axis view was used to measure IVS thickness while M-mode from short axis view was used to measure thickness of left ventricular anterior wall (LVAW) and left ventricular posterior wall (LVPW), and left ventricular internal diameter (LVID). Ejection fraction (EF), fractional shortening (FSN) and left ventricular mass (LVM) were automatically calculated by the Vevo 2100 standard measurement package. Pulsed-wave Doppler images were collected in the apical 4-chamber view to record the mitral Doppler flow spectra. Peak early (E) and late (A) mitral inflow velocities and E/A ratio were measured.

Histological morphology

Hearts were fixed with 10% formalin, dehydrated, and embedded in paraffin. Paraffin-embedded hearts were cut into 4-5 μm sections. Sections were stained with hematoxylin and eosin (H&E) and fluorescein isothiocyanate-conjugated wheat germ agglutinin (WGA) was used to visualize the size of the cardiomyocytes. The immunofluorescence analysis was performed using the standard immunocytochemical techniques. Cross-sectional area of cardiomyocyte was calculated using the Image software.

Cell cultures

The ventricles of neonatal Sprague-Dawley (SD) rats were enzymatically dissociated into cardiomyocytes in PBS containing 0.03% trypsin and 0.04% type II collagenase. Fibroblasts were then removed by a differential attachment technique and the cardiomyocytes were cultivated in DMEM/F12 medium at a density of 2×10^6 cells/well in six-well plates for 24 h. The six-well plates were placed in 37°C, 5% CO_2 incubator. Cells were then washed twice with PBS. In order to evaluate the effect of fructose on cardiomyocyte hypertrophy in vitro, no sugar-DMEM was used and different treatments for 48 h were described as follows: 25 mM glucose in no sugar-DMEM as control; no

sugar-DMEM in the presence of 25 mM glucose and 20 nM SkQ1; 25 mM fructose in no sugar-DMEM; no sugar-DMEM in the presence of 25 mM fructose and 20 nM SkQ1 [15, 22, 23]. The role of ROS in myocardial hypertrophy was confirmed and proved by treating cells with 200 μM H_2O_2 for 48 h [24]. Glucose, fructose, SkQ1 and H_2O_2 were purchased from Sigma. Cell area was measured by confocal microscopy after staining with Alexa Fluor®555 and DIPI (Thermo Fisher, USA).

Adenoviral infection of CFTR shRNA

The adenovirus expressing a small hairpin RNA sequence targeting rat *CFTR* (Adv-shCFTR) was successfully constructed as previously described (Gene ID: 24255, Sunbio Biomedical Technology, China) [25]. The control shRNA (Adv-scr) with no significant homology to any known rat genes was used. Cardiomyocytes were plated in six-well plates and were infected with Adv-shCFTR or Adv-Scr at multiplicity of infection (MOI) of 100 at 37°C. After 2 h, 2 mL of fresh culture media was added and incubated for further 48 h before analysis.

Mitochondria isolation

Heart mitochondria were isolated as previously described [26, 27]. Briefly, heart were rinsed in cold PBS and then homogenized in 2 mL of mitochondria isolation buffer containing protease inhibitor cocktail purchased from Sigma (0.32 M sucrose, 10 mM Tris-HCl, 1 mM EDTA, 2 mM PMSF, PH 7.4) using a Teflon-on-glass electric homogenizer. The homogenate was centrifuged at 1,000 g for 10 minutes at 4°C. The supernatant was then centrifuged at 15,000 g for 15 minutes at 4°C. Isolated mitochondrion were used immediately or frozen at -80°C until use. Protein was quantified with the use of BCA (Pierce, Thermo Fisher Scientific).

ROS detection

The ROS level in heart tissue was estimated using Total ROS Activity Assay Kit (eEnzyme, USA). Hearts were homogenized in ice-cold mitochondria isolation buffer with a Kontes-Duall glass homogenizer. The homogenate was centrifuged at 1,300 × g for 10 min at 4°C to pellet tissue debris and nuclei and the supernatant lysate was used for detection of tissue total ROS. Samples were incubated with Total ROS Green in a 5% CO_2 incubator for 6 hours at 37°C. Fluorescence intensity was monitored at 490 nm excitation and 525 nm emission using fluorescence plate reader.

Mitochondrial H_2O_2 production was measured using the Amplex Ultra Red horseradish peroxidase method (Invitrogen, USA). Mitochondria was diluted in 50 μL of reaction buffer (125 mmol/L KCl, 10 mmol/L HEPES, 5 mmol/L $MgCl_2$, 2 mmol/L K_2HPO_4, pH 7.44) to determine complex I (pyruvate/malate, 5 mmol/L) or complex II (succinate, 5 mmol/L)-driven H_2O_2 production. Fluorescence was followed at an excitation wavelength of 545 nm and an emission wavelength of 590 nm for 20 minutes. The results were reported as picomole per minute per milligram of protein.

Glutathione determination

Mitochondrial reduced glutathione (GSH) and oxidized glutathione (GSSG) were assessed by high performance liquid chromatography (HPLC). Mitochondria pellets were thawed on ice and were lysed by addition of 85 μl of cold water. A 10 μl fraction was kept for protein determination and 10 μl of 40% metaphosphoric acid was added to the remaining lysate. Precipitated protein was eliminated by centrifugation at 17,000 g for 10 min at 4°C. The supernatant was transferred to a chilled glass vial for GSH and GSSG determinations. GSH and GSSG were simultaneously measured by HPLC coupled with ultraviolet (UV) detector (Agilent 1100 Series). Standards and samples were injected with autosampler. The mobile phase (10 mM sodium phosphate, 0.5% methanol, PH=2.7) was delivered at a flow rate of 1 ml/min through a μBONDAPAKTM C18 column (3.9 mm × 30 cm, Waters) placed in an oven at 30°C. Detection was performed at 215 nm by UV detector and typical retention times for GSH and GSSG were 4.3 min and 7.4 min, respectively.

Mitochondria oxygen consumption and ATP production

Oxygen consumption rates were monitored by a Seahorse XF24 oxygen flux analyzer as previously described [26, 27]. Isolated mitochondria were loaded in a 24-well Seahorse plate and 500 μL of ice-cold mitochondrial assay solution (MAS: 70 mmol/L sucrose, 220 mmol/L mannitol, 5 mmol/L KH_2PO_4, 5 mmol/L $MgCl_2$,

2 mmol/L HEPES, 1 mmol/L EGTA, 0.3% BSA fatty acid free, PH 7.4) were added. The 4 sequential ports were injected as following: port A, 50 μL of complex I and complex II substrates and 2.5 mmol/L ADP; port B, 55 μL of 20 μmol/L oligomycin; port C, 60 μL of 40 μmol/L Carbonyl cyanide-4-(trifluoromethoxy) phenylhydrazone (FCCP); and port D 65 μL of 40 μmol/L antimycin A. State III was determined after port A injection, state IV after port B, and uncoupled after port C.

ATP synthesis rates in isolated mitochondria were determined using the luciferin/luciferase-based ATP Bioluminescence Assay Kit HS II (Sigma, USA). Briefly, mitochondria was suspended in 75 μL of buffer A to determine complex I (pyruvate/malate, 5 mmol/L) or complex II (succinate, 5 mmol/L)-driven ATP synthesis. Succinate-driven ATP generation was measured in the presence of complex I inhibitor rotenone to avoid the reverse electron transfer effect [28]. The measurements for all samples were started simultaneously by adding 75 μL of luciferin/luciferase buffer containing 1 mmol/L ADP. The initial slope of the increase in ATP-supported luciferase chemiluminescence was used to determine the rate of ATP production.

Complex II activity measurement

Complex II enzyme activity was measured using microplate assay kit (Abcam, USA). Complex II is immunocaptured within the wells of the microplate. The production of ubiquinol by complex II was coupled to the reduction of the dye DCPIP (2, 6-diclorophenolindophenol) and decreases in its absorbance at 600 nm were measured spectrophotometrically. Enzymatic activity was normalized to mitochondrial protein concentration.

Real-time PCR and western blotting

Total mRNA was isolated from heart tissues or cultured cardiomyocytes using TRIzol reagent (Life Technology, USA). The cDNA was synthesized using the Transcriptor First Strand cDNA Synthesis kit (Life Technology, USA). Quantitative real-time PCR was performed using SYBR Green (Life Technology, USA) and the relative mRNA expressions of atrial natriuretic peptide (ANP, 5'-ACC TGC TAG ACC ACC TGG AG-3', 5'-CCT TGG CTG TTA TCT TCG GTA CCG G-3'), brain natriuretic peptide (BNP, 5'-GAG GTC ACT CCT ATCCTC TGG-3', 5'-GCC ATT TCC TCC GAC TTT TCT C-3') and beta-myosin heavy chain (β-MHC, 5'-CCG AGT CCC AGG TCA ACA A-3', 5'-CTT CAC GGG CAC CCT TGG A-3') were calculated. CFTR primers (Mm00445197_m1) were purchased from Life Technology. GAPDH was measured and used for normalization.

Protein lysates of cardiac tissues and cultured cardiomyocytes were resolved on SDS-PAGE. After transfer to PVDF membrane (Millipore, Bedford, MA, USA), the blot was blocked in TBST (1 mM $CaCl_2$, 136 mM NaCl, 2.5 mM KCl, 25 mM Tris-HCl, 0.1% Tween 20) containing 5% nonfat dry milk and incubated with specific primary antibodies and corresponding secondary antibodies. Rabbit anti-CFTR antibody (H-182, Santa Cruz) were used for immunoblots. Secondary anti-rabbit HRP-linked antibody was purchased from Cell Signaling Technology. GAPDH (Cell Signaling Technology, USA) was used as loading control.

Statistical analysis

Data were presented as mean ± SD. Student's unpaired *t*-test was conducted for comparison between two groups. One-way ANOVA with Bonferroni *post hoc* test was performed for multiple comparisons. All statistical analyses were performed with SPSS software package 20.0 for Windows (Chicago, IL). A value of $P < 0.05$ was considered statistically significant.

Results

SkQ1 attenuated high fructose-induced cardiac hypertrophy and diastolic dysfunction

The potential role of SkQ1 in cardiac hypertrophy and diastolic dysfunction was investigated. The Con mice and SkQ1-treated mice displayed normal echocardiographic images and cardiac morphologies (**Figure 1A** and **1D**). However, high fructose caused changes in echocardiographic images and cardiac morphologies (**Figure 1A** and **1D**). Left ventricular mass index (LVMI) and hypertrophy index (HI) were significantly increased in FS mice (**Figure 1B** and **1C**). Compared with FS mice, SkQ1-treated FS mice had lower LVMI and HI values (**Figure 1B** and **1C**). By H&E and WGA stains, FS mice had greater ventricular cross-sectional area than Con mice and the ventricular cross-sectional area decreased by SkQ1 administra-

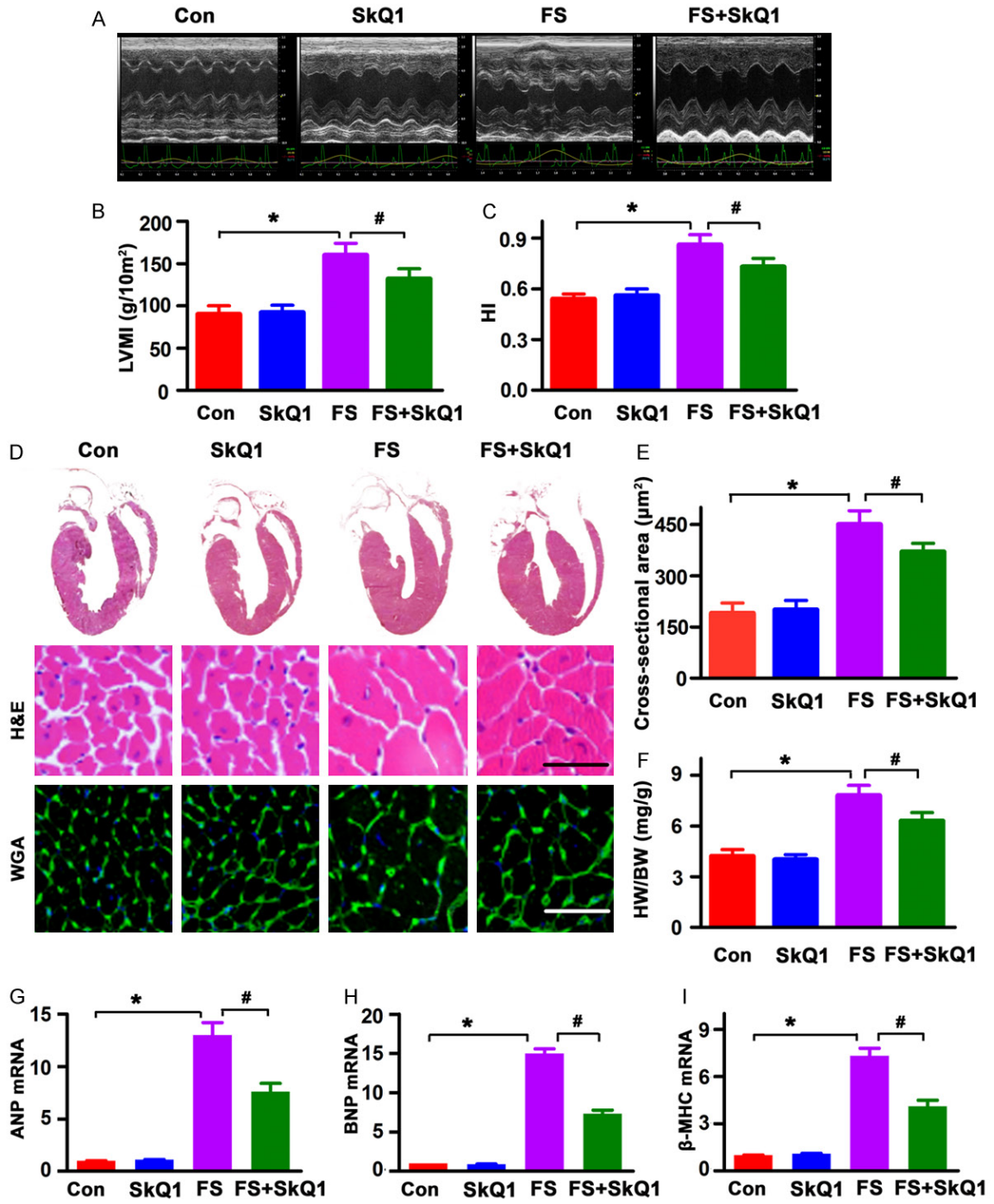

Figure 1. High fructose-induced cardiac hypertrophy was prevented by mitochondrial antioxidant SkQ1. M-mode echocardiographic images of hearts were presented in (A). LVMI was defined as LVM divided by body surface area and HI was calculated as (IVSd+LVPWd)/LVIDd. FS group had increased LVMI and HI but SkQ1 ameliorated the increases in both of them (B and C). Sections of hearts from mice subjected to high fructose and/or SkQ1 feedings were stained with H&E and WGA (scale bar: 50 μm) to analyze cardiac hypertrophy (D). The cross-sectional area of cardiomyocyte was elevated in FS group but SkQ1 prevented the elevation (E). Likewise, SkQ1 caused a reduction in HW/BW of high fructose-fed mice (F). The mRNA levels of cardiac hypertrophic markers were shown in (G-I). Con: control group, SkQ1: SkQ1 group, FS: fructose group, FS+SkQ1: FS+SkQ1 group. HI: hypertrophy index, HW/BW: ratio of heart weight to body weight, IVSd: intraventricular septum in diastole, LVM: left ventricular mass, LVMI: left ventricular mass index, LVPWd: left ventricular posterior wall in diastole, LVIDd: left ventricular inner diameter in diastole. The data were presented as mean ± SD. $^{*}P < 0.05$ vs Con, $^{\#}P < 0.05$ vs FS+SkQ1. n=5-12 for each group.

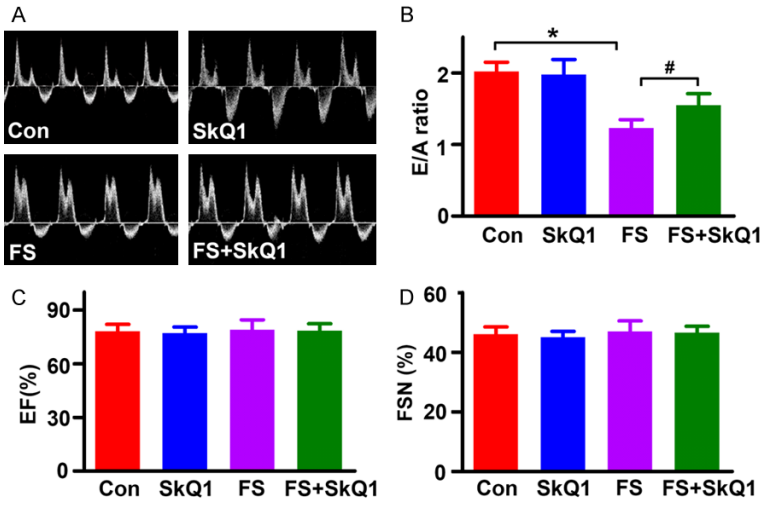

Figure 2. High fructose induced changes in cardiac diastolic and systolic functions. Left ventricular diastolic function was assessed by transmitral flow velocity (A). High fructose significantly affected cardiac diastolic function which was preserved in FS+SkQ1 group (B). Systolic function was also evaluated and the parameters of EF and FSN were recorded. The data indicated that fructose did not change myocardial contraction (C and D). Con: control group, SkQ1: SkQ1 group, FS: fructose group, FS+SkQ1: fructose+SkQ1 group. EF: ejection fraction, FSN: fractional shortening. The data were presented as mean ± SD. $^{*}P < 0.05$ vs Con, $^{\#}P < 0.05$ vs FS+SkQ1. n=5-12 for each group.

tion (**Figure 1E**). As shown in **Figure 1F**, heart size assessed as the ratio of heart weight to body weight (HW/BW) tended to be largest in FS group but SkQ1 attenuated the increased HW/BW ratio, which indicated SkQ1 application inhibited the process of high fructose-induced cardiac hypertrophy. We measured the mRNA levels of cardiac hypertrophic markers (ANP, BNP, and β-MHC) and our results revealed increases in their levels after 20-week high fructose feeding (**Figure 1G-I**).

Cardiac function was evaluated by echocardiography and Doppler. E peak reflected the blood flow velocity of mitral valves in early diastole while A peak presented the blood flow velocity of mitral valves in late diastole (**Figure 2A**). Our results showed that high fructose led to decreased E/A ratio which suggested that long-term high fructose feeding caused left ventricular diastolic dysfunction (**Figure 2B**). However, high fructose-induced left ventricular diastolic dysfunction was improved by SkQ1 (**Figure 2B**). Although high fructose affected diastolic function, there were no changes in EF and FSN after 20-week high fructose feeding (**Figure 2C** and **2D**).

Mitochondrial ROS mediated high fructose-induced myocardial hypertrophy

Compared with Con group, total ROS level in cardiac tissue from FS group was increased by 80% and SkQ1 administration prevented the increase in total ROS level (**Figure 3A**). In cardiac mitochondria from FS mice, H_2O_2 production was increased with either complex I or complex II substrates (**Figure 3B**). The fructose-induced increase in mitochondrial H_2O_2 productions with both complex I and II substrates were ameliorated by SkQ1 (**Figure 3B**). Mitochondrial GSH/GSSG ratio tended to be lowest in FS group but SkQ1 treatment partly preserved the mitochondrial GSH/GSSG ratio (**Figure 3C**).

In order to investigate the critical role of mitochondrial ROS in fructose-induced myocardial hypertrophy, we cultured cardiomyocytes of neonatal SD. Firstly, we used fructose to treat cells and observed whether fructose caused cardiomyocyte hypertrophy in vitro. The results showed that fructose led to hypertrophic morphology of cardiomyocyte meanwhile cell area was increased by fructose treatment (**Figure 3D** and **3E**). In addition, fructose led to increased mitochondrial H_2O_2 production (**Figure 3F**). However, SkQ1 prevented fructose-induced cardiomyocyte hypertrophy and increased mitochondrial H_2O_2 production (**Figure 3D-F**), which was consistent to in vivo data. Then we confirmed ROS-mediated cardiomyocyte hypertrophy using exogenous H_2O_2 and the antioxidant function of SkQ1 against H_2O_2 (**Figure 3G** and **3H**).

Mitochondrial respiratory chain function was impaired by high fructose

High fructose decreased complex II activity by 60% and SkQ1 restored complex II activity in vivo (**Figure 4A**). State III and IV oxygen consumption rates with complex I substrate reduced in fructose-fed mice but SkQ1 adminis-

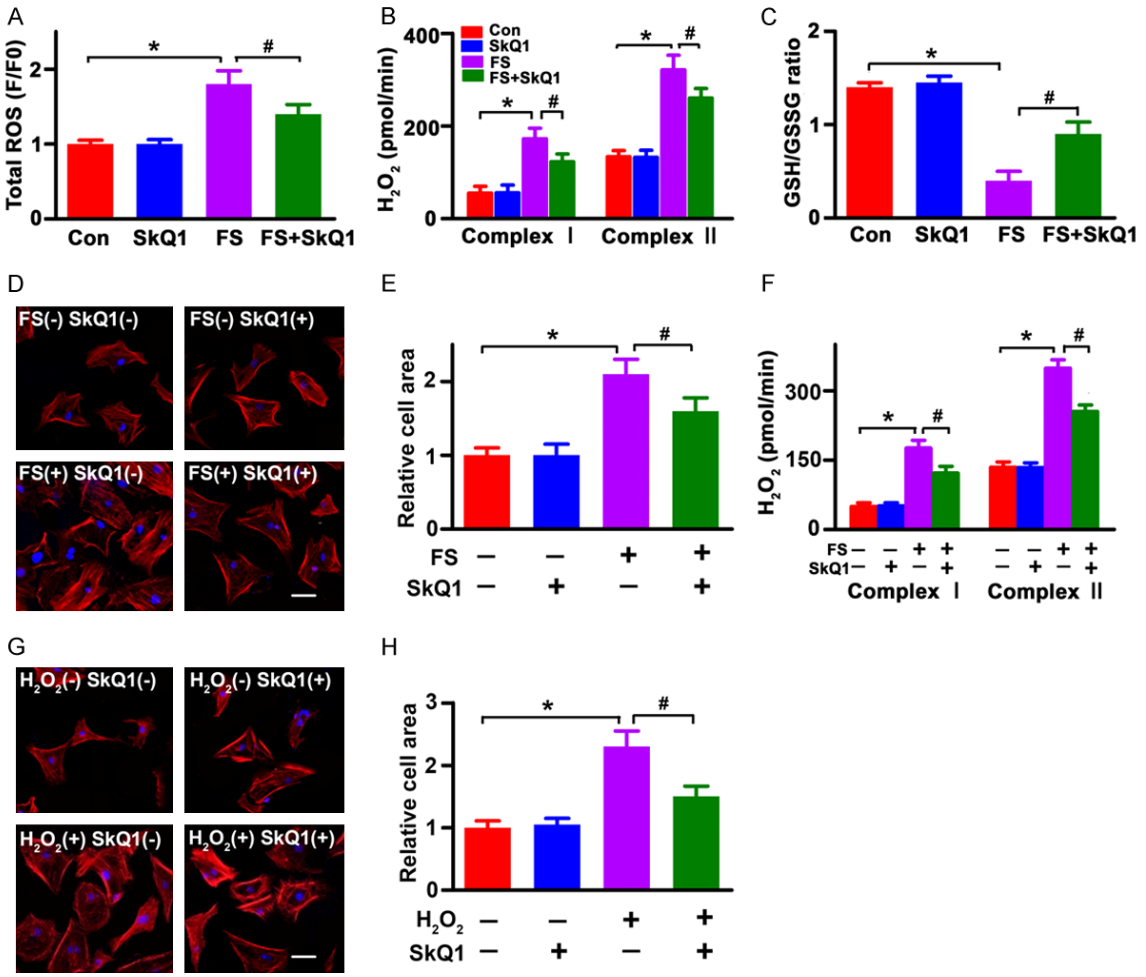

Figure 3. Mitochondrial ROS mediated high fructose-induced myocardial hypertrophy. A-C: By in vivo study, total ROS and mitochondrial H_2O_2 production were significantly increased in FS group but SkQ1 prevented high fructose-induced elevations in both of them. As an antioxidant indicator, GSH/GSSG ratio was reduced by high fructose feeding while partially restored in FS+SkQ1 group. Con: control group, SkQ1: SkQ1 group, FS: fructose group, FS+SkQ1: FS+SkQ1 group. GSH: reduced glutathione, GSSG: oxidized glutathione, ROS: reactive oxygen species. *P < 0.05 vs Con, #P < 0.05 vs FS+SkQ1. n=5-12 for each group. D-F: By in vitro experiment, cardiomyocyte exhibited hypertrophic morphology and cell area significantly increased in response to 25 mM fructose treatment for 48 h but cardiomyocyte hypertrophy was partially preserved by 20 nM SkQ1 administration (sale bar: 50 μm). Mitochondrial H_2O_2 production of cardiomyocytes treated with 25 mM fructose for 48 h was faster than that of cardiomyocytes with 25 mM glucose but 20 nM SkQ1 application retarded the mitochondrial H_2O_2 production of cardiomyocytes treated with fructose. *P < 0.05 vs FS (-) & SkQ1 (-), #P < 0.05 vs FS (+) & SkQ1 (+). n=5. G, H: Treatment with 200 μM H_2O_2 for 48 h led to cardiomyocyte hypertrophy in vitro while SkQ1 scavenged H_2O_2 to inhibit cardiomyocyte hypertrophy (sale bar: 50 μm). *P < 0.05 vs H_2O_2 (-) & SkQ1 (-), #P < 0.05 vs H_2O_2 (+) & SkQ1 (+). n=5.

tration partly preserved oxygen consumption rates (**Figure 4B** and **4C**). Complex II-mediated state III and state IV oxygen consumption rates were significantly decreased in FS group but the reductions in both state III and state IV oxygen consumption rates were prevented in FS+SkQ1 group (**Figure 4B** and **4C**). In mitochondria from FS mice, ATP synthesis rates were decreased by 37% and 36% for complex I and complex II substrates, respectively (**Figure 4D**). The fructose-induced decreases in ATP synthesis rates for both complex I and complex II substrates were prevented by SkQ1 (**Figure 4D**).

Loss of CFTR contributed to mitochondrial oxidative stress in high fructose-induced myocardial hypertrophy

Quantitative real-time PCR and western blotting assays showed that cardiac CFTR expressions were decreased in FS group compared

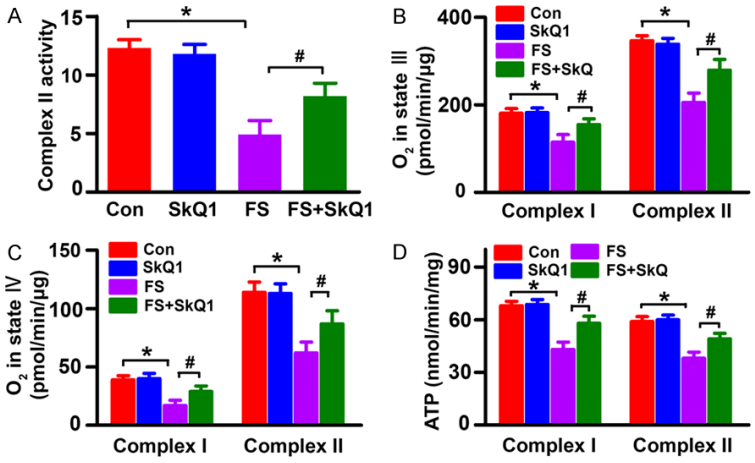

Figure 4. High fructose impaired mitochondrial respiration chain function. High fructose-fed mice exhibited decreased complex II activity which was partly corrected by SkQ1 administration (A). Maximal oxygen consumption rates in state III and uncoupled oxygen consumption rates in state IV driven by complex I and II substrates were decreased in high fructose-fed mice but preserved in SkQ1-treated mice with high fructose feeding (B and C). Decreases in complex I and II substrate-driven cardiac mitochondrial ATP synthesis rates were prevented by SkQ1 (D). Con: control group, SkQ1: SkQ1 group, FS: fructose group, FS+SkQ1: FS+SkQ1 group. The data were presented as mean ± SD. $^*P < 0.05$ vs Con, $^\#P < 0.05$ vs FS+SkQ1. n=5-12 for each group.

with Con group (**Figure 5A** and **5B**). SkQ1 administration did not influence CFTR protein and mRNA expressions (**Figure 5A** and **5B**). We used Adv-shCFTR to infect cardiomyocytes to reveal whether CFTR regulated mitochondrial ROS production. Adv-shCFTR infection successfully disrupted CFTR expression which caused significant increases in mitochondrial H_2O_2 production and mRNA levels of myocardial hypertrophic markers (**Figure 5C-G**). Taken together, in vivo and in vitro findings suggested that high fructose caused mitochondrial oxidative stress by regulating CFTR expression.

Discussion

In the present study, we confirmed that long-term high fructose diet resulted in cardiac hypertrophy and diastolic dysfunction. The production of ROS elevated in cardiac mitochondria after the initiation of a fructose-enriched diet. Both in vitro and in vivo experiments proved that mitochondrial oxidative stress was a key event and mediated the development of cardiac hypertrophy. High fructose diet reduced CFTR expression and CFTR silence enhanced mitochondrial ROS production, which suggested high fructose led to mitochondrial oxidative stress by regulating CFTR expression. The mechanism for impaired electron transport chain may be linked to mitochondrial oxidative stress.

Epidemiological studies have reported that a Western diet containing high-fat and high-fructose is strongly associated with the increasing prevalence of cardiovascular disease [29]. A study by Kimberley Mellor *et al* indicated that long-term 12-week high fructose intake induced apparent ventricular hypertrophy but 6-week high fructose diet failed to cause cardiac hypertrophy [30, 31]. Their study also demonstrated that elevated myocardial superoxide production preceded the cardiac hypertrophic response to a high fructose diet in mice [30, 31]. In our study, mice were fed high fructose for 20 weeks and exhibited significant cardiac hypertrophy and diastolic dysfunction. Both total ROS and mitochondrial H_2O_2 production elevated in hearts from mice following long-term high fructose intake. Fructose-induced hypertrophic cardiomyocyte was also confirmed in vitro and mitochondrial H_2O_2 production rate in cardiomyocyte with fructose treatment became faster in the present study. It is well known that ROS plays a central role in LVH and diastolic dysfunction [1, 9]. Numerous studies have reported that exogenous ROS can modulate signaling pathways involved in cardiomyocyte hypertrophy, such as the activation of ERK1/2, JNK, and PKCs [32]. We used H_2O_2 to treat cardiomyocyte and found the cell area was enlarged, which is consistent with previous studies [24, 33-35].

It is urgent to answer whether mitochondrial oxidative stress mediates high fructose-induced cardiac hypertrophy, since mitochondrial H_2O_2 production rate was markedly increased following high fructose intake in this study. Until now, there are no evidence concerning involvement of mitochondrial ROS in high fructo-

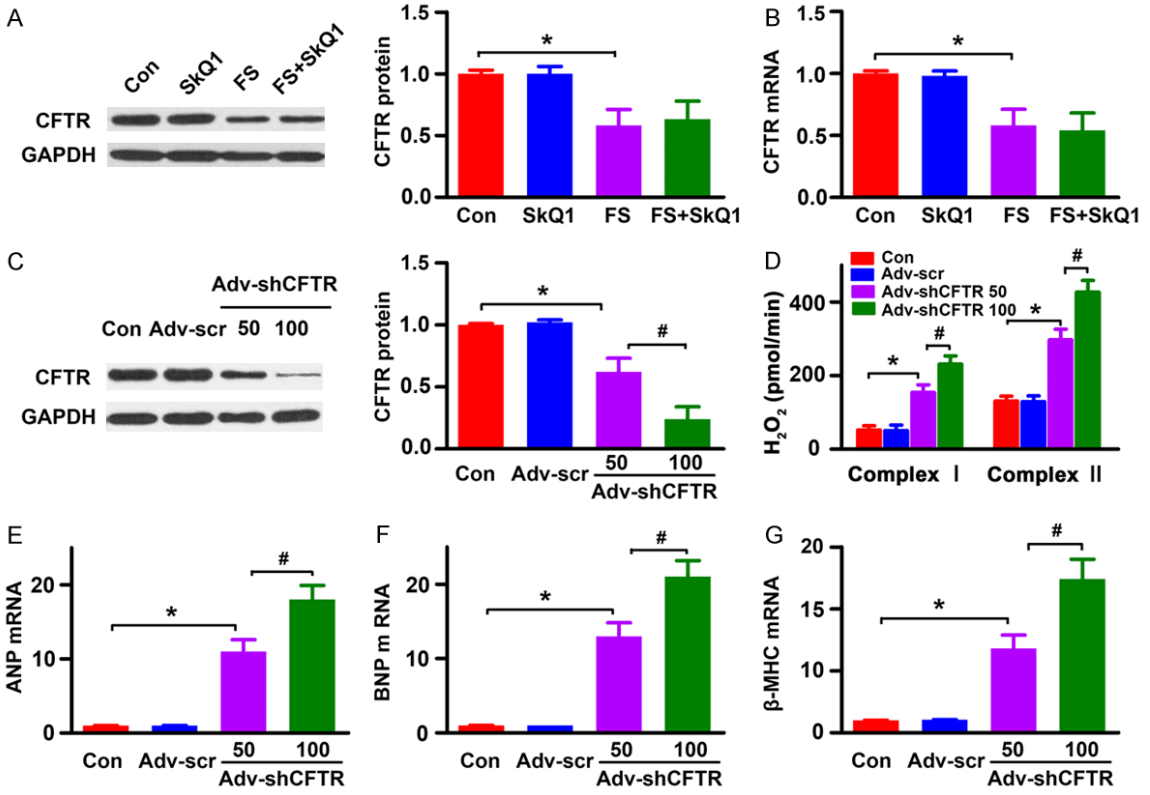

Figure 5. CFTR regulated mitochondrial ROS in high fructose-induced myocardial hypertrophy. A, B: By in vivo study, the expressions of CFTR protein and mRNA were reduced in heats from FS group. There was no difference in CFTR expressions between FS and FS+SkQ1 groups. Con: control group, SkQ1: SkQ1 group, FS: fructose group, FS+SkQ1: FS+SkQ1 group. *$P < 0.05$ vs Con. n=5-12 for each group. C-G: Infection with Adv-shCFTR at concentrations of 50 MOI and 100 MOI for 48 h significantly decreased endogenous CFTR expression and infection with adenovirus containing scrambled sequence (Adv-scr) did not affect CFTR expression in cultured cardiomyoctes. With the Adv-shCFTR infection, mitochondrial H_2O_2 production was significantly increased. Meanwhile, the mRNA levels of myocardial hypertrophic markers also elevated because of CFTR silence. *$P < 0.05$ vs Con, #$P < 0.05$ vs Adv-shCFTR 100. n=5.

se-induced heart hypertrophy. Recently, mitochondria-targeted antioxidant SkQ1 has been developed and allows us to detect the role of mitochondrial oxidative stress in various pathological processes. SkQ1 is the most effective protector to reduce the intensity of pathological processes connected with ROS generation in tens of models both in vivo and in vitro [36]. Lipophilic cation SkQ1 could penetrate mitochondrial membrane and protect mitochondria from oxidative damage by scavenging superoxide [36-38]. Our data showed that SkQ1 not only attenuated high fructose-induced cardiac hypertrophy in mice but also ameliorated enlarged cell area of cardiomyocyte induced by high fructose in vitro, which supports that high fructose leads to cardiac hypertrophy via mitochondrial oxidative stress. It should be noted that a critical role of mitochondrial ROS in mediating myocardial hypertrophy and diastolic dysfunction has been raised by many studies [1, 39, 40]. Aaron L. Sverdlov *et al* used transgenic mice overexpressing catalase in mitochondria to prove that mitochondrial ROS played an important role in high-fat high-sucrose induced LVH and diastolic dysfunction [1].

ROS are thought to be generated at electron transport chain through leakage during respiration and there is cross talk between the redox couples and electron transport chain.

Complex II, consisting of 4 nuclear-encoded proteins-SDHA, SDHB, SDHC and SDHD, couples the oxidation of succinate to fumarate in the matrix [41, 42]. It has been previously identified that Cys100 and Cys103 in SHDB underwent reversible oxidative modification in mice fed high-fat high-sucrose diet [9]. The cysteine-

to-serine mutation of either Cys100 or Cys103 protected against H_2O_2-induced decrease in complex II activity in HEK cells [1]. Reduced complex II activity, as well as O_2 consumption and ATP production abnormalities, were observed in FS mice and partially prevented by mitochondrial-targeted antioxidant SkQ1 in our study. Our finding suggests that respiratory chain dysfunction is involved in high fructose-induced cardiac hypertrophy and increased mitochondrial ROS may contribute to respiratory chain damage.

CFTR protein, which functions as a chloride channel within various cells and tissues, represents an organic anion efflux channel that is permeable to Cl^- and other larger organic ions [43]. It also functions as a regulator of other ion channels, principally the epithelial Na^+ and HCO_3^- channels [43]. Mutation of *CFTR* gene reduces the channel function and leads to cystic fibrosis (CF). A previous study showed that mitochondrial-derived oxidative stress was apparent in CFTR knockout mice and it revealed that mitochondrial GSH was significantly lower in lungs from mice lacking a functional CFTR protein [18]. Oxidative stress may be a result of a decreased availability of GSH to neutralize endogenous ROS generation in CFTR knockout mice [18]. We observed decreased CFTR expression, reduced mitochondrial GSH: GSSG ratio and increased mitochondrial H_2O_2 production rate in high fructose-fed mice. By adv-shCFTR infection, CFTR silence increased H_2O_2 production rate and caused oxidative stress in mitochondria. Those results support high fructose induces mitochondrial oxidative stress by regulating CFTR expression.

Collectively, these findings indicated that high fructose successfully induced cardiac hypertrophy model and led to cardiac diastolic dysfunction in mice. Mitochondrial oxidative stress mediated cardiac hypertrophy and diastolic dysfunction induced by high fructose intervention. The present study provides new insights into the regulation mechanisms of high fructose-induced cardiac hypertrophy. CFTR expression preservation and specific antioxidant for mitochondrial ROS may be of value for the treatment of high fructose-induced cardiac hypertrophy. The mechanism by which respiratory chain is impaired in high fructose model remains to be determined in further research.

Acknowledgements

This study was supported by the National Natural Science Foundation of China (No. 81371-443 and No. 81400305), Beijing Talents Fund (No. 2014000021469G233), Beijing Natural Science Foundation (No. 7152045, No. 7122-056, No. 7142049 and No. 7142137), Beijing Municipal Administration of Hospitals Incubating Program (No. PX2016046), Basic and Clinical Research Foundation of Capital Medical University (No. 13JL26), Natural Science Foundation of Xinjiang (No. 2014211A063) and Beijing Municipal Health Bureau High-Level Talent Cultivation (No. 2014-3-043).

Disclosure of conflict of interest

None.

Address correspondence to: Dr. Yan-Bo Zhang, Research Center of Cardiovascular Diseases, State Key Laboratory of Cardiovascular Disease, Fuwai Hospital, National Center for Cardiovascular Diseases, Chinese Academy of Medical Sciences and Peking Union Medical College, 167 Bei-Li-Shi Road, Beijing 100037, People's Republic of China. Tel: (86)-18600372914; Fax: (86)-01088396614; E-mail: mmclis@sina.com

References

[1] Sverdlov AL, Elezaby A, Qin F, Behring JB, Luptak I, Calamaras TD, Siwik DA, Miller EJ, Liesa M, Shirihai OS, Pimentel DR, Cohen RA, Bachschmid MM, Colucci WS. Mitochondrial Reactive Oxygen Species Mediate Cardiac Structural, Functional, and Mitochondrial Consequences of Diet-Induced Metabolic Heart Disease. J Am Heart Assoc 2016; 5.

[2] Mells JE, Fu PP, Sharma S, Olson D, Cheng L, Handy JA, Saxena NK, Sorescu D, Anania FA. Glp-1 analog, liraglutide, ameliorates hepatic steatosis and cardiac hypertrophy in C57BL/6J mice fed a Western diet. Am J Physiol Gastrointest Liver Physiol 2012; 302: G225-235.

[3] Zhang J, Zhang BH, Yu YR, Tang CS, Qi YF. Adrenomedullin protects against fructose-induced insulin resistance and myocardial hypertrophy in rats. Peptides 2011; 32: 1415-1421.

[4] Bouchard-Thomassin AA, Lachance D, Drolet MC, Couet J, Arsenault M. A high-fructose diet worsens eccentric left ventricular hypertrophy in experimental volume overload. Am J Physiol Heart Circ Physiol 2011; 300: H125-134.

[5] Chess DJ, Xu W, Khairallah R, O'Shea KM, Kop WJ, Azimzadeh AM, Stanley WC. The antioxi-

dant tempol attenuates pressure overload-induced cardiac hypertrophy and contractile dysfunction in mice fed a high-fructose diet. Am J Physiol Heart Circ Physiol 2008; 295: H2223-2230.
[6] Santos CX, Anilkumar N, Zhang M, Brewer AC, Shah AM. Redox signaling in cardiac myocytes. Free Radic Biol Med 2011; 50: 777-793.
[7] Murphy MP. How mitochondria produce reactive oxygen species. Biochem J 2009; 417: 1-13.
[8] Ku HJ, Ahn Y, Lee JH, Park KM, Park JW. IDH2 deficiency promotes mitochondrial dysfunction and cardiac hypertrophy in mice. Free Radic Biol Med 2015; 80: 84-92.
[9] Sverdlov AL, Elezaby A, Behring JB, Bachschmid MM, Luptak I, Tu VH, Siwik DA, Miller EJ, Liesa M, Shirihai OS, Pimentel DR, Cohen RA, Colucci WS. High fat, high sucrose diet causes cardiac mitochondrial dysfunction due in part to oxidative post-translational modification of mitochondrial complex II. J Mol Cell Cardiol 2015; 78: 165-173.
[10] Al-Awwadi NA, Araiz C, Bornet A, Delbosc S, Cristol JP, Linck N, Azay J, Teissedre PL, Cros G. Extracts enriched in different polyphenolic families normalize increased cardiac NADPH oxidase expression while having differential effects on insulin resistance, hypertension, and cardiac hypertrophy in high-fructose-fed rats. J Agric Food Chem 2005; 53: 151-157.
[11] Miatello R, Vazquez M, Renna N, Cruzado M, Zumino AP, Risler N. Chronic administration of resveratrol prevents biochemical cardiovascular changes in fructose-fed rats. Am J Hypertens 2005; 18: 864-870.
[12] Adlam VJ, Harrison JC, Porteous CM, James AM, Smith RA, Murphy MP, Sammut IA. Targeting an antioxidant to mitochondria decreases cardiac ischemia-reperfusion injury. FASEB J 2005; 19: 1088-1095.
[13] Lowes DA, Thottakam BM, Webster NR, Murphy MP, Galley HF. The mitochondria-targeted antioxidant MitoQ protects against organ damage in a lipopolysaccharide-peptidoglycan model of sepsis. Free Radic Biol Med 2008; 45: 1559-1565.
[14] Gioscia-Ryan RA, LaRocca TJ, Sindler AL, Zigler MC, Murphy MP, Seals DR. Mitochondria-targeted antioxidant (MitoQ) ameliorates age-related arterial endothelial dysfunction in mice. J Physiol 2014; 592: 2549-2561.
[15] Demyanenko IA, Popova EN, Zakharova VV, Ilyinskaya OP, Vasilieva TV, Romashchenko VP, Fedorov AV, Manskikh VN, Skulachev MV, Zinovkin RA, Pletjushkina OY, Skulachev VP, Chernyak BV. Mitochondria-targeted antioxidant SkQ1 improves impaired dermal wound healing in old mice. Aging (Albany NY) 2015; 7: 475-485.
[16] Plotnikov EY, Silachev DN, Jankauskas SS, Rokitskaya TI, Chupyrkina AA, Pevzner IB, Zorova LD, Isaev NK, Antonenko YN, Skulachev VP, Zorov DB. Mild uncoupling of respiration and phosphorylation as a mechanism providing nephro- and neuroprotective effects of penetrating cations of the SkQ family. Biochemistry (Mosc) 2012; 77: 1029-1037.
[17] Plotnikov EY, Chupyrkina AA, Jankauskas SS, Pevzner IB, Silachev DN, Skulachev VP, Zorov DB. Mechanisms of nephroprotective effect of mitochondria-targeted antioxidants under rhabdomyolysis and ischemia/reperfusion. Biochim Biophys Acta 2011; 1812: 77-86.
[18] Velsor LW, Kariya C, Kachadourian R, Day BJ. Mitochondrial oxidative stress in the lungs of cystic fibrosis transmembrane conductance regulator protein mutant mice. Am J Respir Cell Mol Biol 2006; 35: 579-586.
[19] Kelly-Aubert M, Trudel S, Fritsch J, Nguyen-Khoa T, Baudouin-Legros M, Moriceau S, Jeanson L, Djouadi F, Matar C, Conti M, Ollero M, Brouillard F, Edelman A. GSH monoethyl ester rescues mitochondrial defects in cystic fibrosis models. Hum Mol Genet 2011; 20: 2745-2759.
[20] Zhou JJ, Wei Y, Zhang L, Zhang J, Guo LY, Gao C, Li DP, Zhang Y. Chronic intermittent hypobaric hypoxia prevents cardiac dysfunction through enhancing antioxidation in fructose-fed rats. Can J Physiol Pharmacol 2013; 91: 332-337.
[21] Vinhas M, Araujo AC, Ribeiro S, Rosario LB, Belo JA. Transthoracic echocardiography reference values in juvenile and adult 129/Sv mice. Cardiovasc Ultrasound 2013; 11: 12.
[22] Pazzini CE, Colpo AC, Poetini MR, Pires CF, de Camargo VB, Mendez AS, Azevedo ML, Soares JC, Folmer V. Effects of Red Wine Tannat on Oxidative Stress Induced by Glucose and Fructose in Erythrocytes in Vitro. Int J Med Sci 2015; 12: 478-486.
[23] Zhao L, Guo X, Wang O, Zhang H, Wang Y, Zhou F, Liu J, Ji B. Fructose and glucose combined with free fatty acids induce metabolic disorders in HepG2 cell: A new model to study the impacts of high-fructose/sucrose and high-fat diets in vitro. Mol Nutr Food Res 2016; 60: 909-921.
[24] Zhao M, Guo H, Chen J, Fujino M, Ito H, Takahashi K, Abe F, Nakajima M, Tanaka T, Wang J, Huang H, Zheng S, Hei M, Li J, Ma X, Chen Y, Zhao L, Zhuang J, Zhu P, Li XK. 5-aminolevulinic acid combined with sodium ferrous citrate ameliorates H2O2-induced cardiomyocyte hypertrophy via activation of the MAPK/Nrf2/HO-1 pathway. Am J Physiol Cell Physiol 2015; 308: C665-672.
[25] Zeng JW, Zeng XL, Li FY, Ma MM, Yuan F, Liu J, Lv XF, Wang GL, Guan YY. Cystic Fibro-

sis Transmembrane Conductance Regulator (CFTR) prevents apoptosis induced by hydrogen peroxide in basilar artery smooth muscle cells. Apoptosis 2014; 19: 1317-1329.

[26] Elezaby A, Sverdlov AL, Tu VH, Soni K, Luptak I, Qin F, Liesa M, Shirihai OS, Rimer J, Schaffer JE, Colucci WS, Miller EJ. Mitochondrial remodeling in mice with cardiomyocyte-specific lipid overload. J Mol Cell Cardiol 2015; 79: 275-283.

[27] Liesa M, Luptak I, Qin F, Hyde BB, Sahin E, Siwik DA, Zhu Z, Pimentel DR, Xu XJ, Ruderman NB, Huffman KD, Doctrow SR, Richey L, Colucci WS, Shirihai OS. Mitochondrial transporter ATP binding cassette mitochondrial erythroid is a novel gene required for cardiac recovery after ischemia/reperfusion. Circulation 2011; 124: 806-813.

[28] Sahin E, Colla S, Liesa M, Moslehi J, Muller FL, Guo M, Cooper M, Kotton D, Fabian AJ, Walkey C, Maser RS, Tonon G, Foerster F, Xiong R, Wang YA, Shukla SA, Jaskelioff M, Martin ES, Heffernan TP, Protopopov A, Ivanova E, Mahoney JE, Kost-Alimova M, Perry SR, Bronson R, Liao R, Mulliqan R, Shirihai OS, Chin L, Depinho RA. Telomere dysfunction induces metabolic and mitochondrial compromise. Nature 2011; 470: 359-365.

[29] Remig V, Franklin B, Margolis S, Kostas G, Nece T, Street JC. Trans fats in America: a review of their use, consumption, health implications, and regulation. J Am Diet Assoc 2010; 110: 585-592.

[30] Mellor K, Ritchie R, Morris M, Delbridge L. Elevated myocardial superoxide production precedes the cardiac hypertrophy response to a high fructose diet in mice. Am J Physiol Renal Physiol 2016; 310: F547-559.

[31] Mellor K, Ritchie RH, Meredith G, Woodman OL, Morris MJ, Delbridge LM. High-fructose diet elevates myocardial superoxide generation in mice in the absence of cardiac hypertrophy. Nutrition 2010; 26: 842-848.

[32] Sugden PH, Clerk A. Oxidative stress and growth-regulating intracellular signaling pathways in cardiac myocytes. Antioxid Redox Signal 2006; 8: 2111-2124.

[33] Liu L, Li J, Liu J, Yuan Z, Pierre SV, Qu W, Zhao X, Xie Z. Involvement of Na+/K+-ATPase in hydrogen peroxide-induced hypertrophy in cardiac myocytes. Free Radic Biol Med 2006; 41: 1548-1556.

[34] Foussal C, Lairez O, Calise D, Pathak A, Guilbeau-Frugier C, Valet P, Parini A, Kunduzova O. Activation of catalase by apelin prevents oxidative stress-linked cardiac hypertrophy. FEBS Lett 2010; 584: 2363-2370.

[35] Seenarain V, Viola HM, Ravenscroft G, Casey TM, Lipscombe RJ, Ingley E, Laing NG, Bringans SD, Hool LC. Evidence of altered guinea pig ventricular cardiomyocyte protein expression and growth in response to a 5 min in vitro exposure to H(2)O(2). J Proteome Res 2010; 9: 1985-1994.

[36] Chistyakov VA, Prazdnova EV, Gutnikova LV, Sazykina MA, Sazykin IS. Superoxide scavenging activity of plastoquinone derivative 10-(6'-plastoquinonyl) decyltriphenylphosphonium (SkQ1). Biochemistry (Mosc) 2012; 77: 776-778.

[37] Khailova LS, Dedukhova VI, Mokhova EN. Cations SkQ1 and MitoQ accumulated in mitochondria delay opening of ascorbate/FeSO4-induced nonspecific pore in the inner mitochondrial membrane. Biochemistry (Mosc) 2008; 73: 1121-1124.

[38] Popova EN, Pletjushkina OY, Dugina VB, Domnina LV, Ivanova OY, Izyumov DS, Skulachev VP, Chernyak BV. Scavenging of reactive oxygen species in mitochondria induces myofibroblast differentiation. Antioxid Redox Signal 2010; 13: 1297-1307.

[39] Qin F, Siwik DA, Luptak I, Hou X, Wang L, Higuchi A, Weisbrod RM, Ouchi N, Tu VH, Calamaras TD, Miller EJ, Verbeuren TJ, Walsh K, Cohen RA, Colucci WS. The polyphenols resveratrol and S17834 prevent the structural and functional sequelae of diet-induced metabolic heart disease in mice. Circulation 2012; 125: 1757-1764, S1751-1756.

[40] Wu R, Wyatt E, Chawla K, Tran M, Ghanefar M, Laakso M, Epting CL, Ardehali H. Hexokinase II knockdown results in exaggerated cardiac hypertrophy via increased ROS production. EMBO Mol Med 2012; 4: 633-646.

[41] Wojtovich AP, Smith CO, Haynes CM, Nehrke KW, Brookes PS. Physiological consequences of complex II inhibition for aging, disease, and the mKATP channel. Biochim Biophys Acta 2013; 1827: 598-611.

[42] Yankovskaya V, Horsefield R, Tornroth S, Luna-Chavez C, Miyoshi H, Leger C, Byrne B, Cecchini G, Iwata S. Architecture of succinate dehydrogenase and reactive oxygen species generation. Science 2003; 299: 700-704.

[43] Zhang YP, Zhang H, Duan DD. Chloride channels in stroke. Acta Pharmacol Sin 2013; 34: 17-23.